

Chapter 3

Utilization of Solar Energy and Bio-Energy in Oil industry

3.1 Introduction

The previous chapter has dealt with Solar Energy and Bio-Energy for carbon emission mitigation and adaptation. The mathematical modeling of PV module and its performance has been explained. Utilizing MATLAB simulation for the compatibility of solar power with grid electricity has been briefed. Second scenario of Concentrated Solar Power technology (CSP) has been projected for industrial applications. Third and interdisciplinary approach of micro-algae based Carbon sequestration has been firmed up for reducing the CO₂ emissions from industrial vents.

This chapter details about specific multidisciplinary research studies at ONGC for different industrial applications as briefed under:

- a) Solar Photovoltaic energy optimization for a Natural Gas (NG) fed **Captive Power Plant (CPP)** at Location 1.
- b) Substitution of Natural Gas with CSP for crude oil heating applications at **Group Gathering Station (GGS)** at Location 2.
- c) Bio-fixation of Greenhouse Gases (GHG)-CO₂ with microalgae at a **Gas Processing Complex** at Location 3.

3.2 Solar Energy Optimization at Captive Power Plant-Assam

The research idea is to utilize the optimized solar electricity at industrial location 1 with a unique 'Despatcher' based control system. The control system maximizes the use of solar electricity and reduces the consumption of grid electricity. The unique despatcher model has been developed based on appropriate stochastic models.

The optimization of solar power has been modeled for 6 MW power plant at location 1, which feeds the electrical power to various installations in Oil and Gas field of Geleky ONGC Assam. The power plant is based on NG fed turbines and running round the clock and responsible for about 80% of power requirement. The schematic of CPP and its customers (Installations of oil field) has been shown in the Figure 3.1. The power generation is at 11 kV level and then supplied to various associated installations.

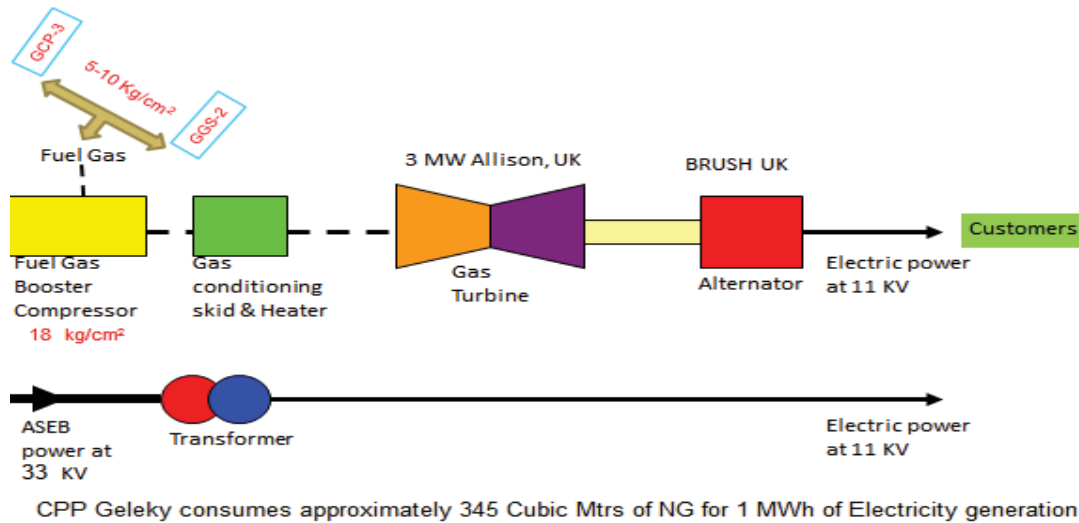


Figure. 3.1. Schematic of Captive Power Plant(CPP) at location 1

There are other auxiliary systems like fuel gas booster compressors, cooling water pumps, cooling towers, air compressors, fire and gas systems, battery banks, and switchgear system. Other safety and utility systems include fire water pump & sprinkler system, firefighting equipment, and bore well. The plant operation is being monitored from the control room.

3.2.1. Description of the Control system

The primary approach of present work is to design a Dispatcher system which controls the plant's essential devices to have option to use solar electricity or grid electricity based on prediction of dynamic weather conditions. The concept, design and methodology of the control system have been discussed.

The balance between solar generation and consumption has been derived utilizing a MATLAB based software program. This balancing would provide reserve power and it means that the starting of the equipment ON and OFF based on users using 'Solar Power Generation Prognosis'. It refers that non-essential devices will start their work when the generation covers their needs and essential devices would continuously work on grid power and solar power.

The dispatcher makes decisions about devices work time-based on the device and external parameters. As such various devices/ equipment used in at location 1 has been divided into two groups, first group as service devices, which service permanent plant needs, such as Battery Chargers, Cooling water system, Programmable Logic Control (PLC) etc, and second group devices, which

service variable inconsistent owner needs, such devices as Booster compressors, Low Pressure (LP)/ High Pressure (HP) Gas compressors, etc.

The first group of devices has been controlled by the reference to sensors which measure value with an allowed range. Time of work cycle for such devices is small, e.g., by the one-second pump will move some water or air from one place to other. The decisions have been made based on the instantaneous data.

The second group of devices has a corresponding long work cycle which cannot be stopped at any moment and power generation forecast horizon is longer than its work cycle to make possible choosing of the most cost-efficient work period. This includes a module called ‘Solar power prognosis’, which propagates solar panels electricity generation for all light day and deliver estimated energy values for every minute. The system includes third module for uncontrolled energy consumption propagation and block diagram for despatcher system has been presented in Figure. 3.2.

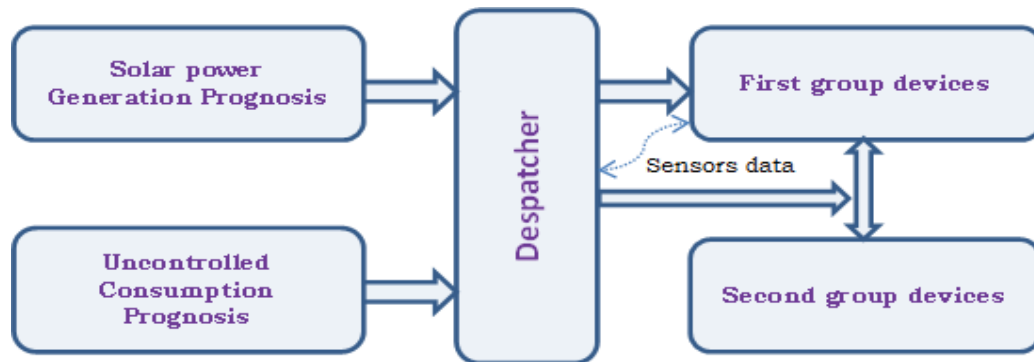


Figure. 3.2. Control system block diagram.

All data pertaining to solar power generation, and uncontrolled consumption, essential/ nonessential equipment, and work-time, shall be provided through controlled sensor feedback as shown in Figure 3.2 between despatcher and first group devices for the modeling system. The estimation of solar electrical power needs geographical data with time fluctuating sun intensity, position, weather conditions and panel efficiency.

3.2.2. Solar Plant Energy Generation Prognosis

For the estimation of data, a solar panel installed near to location 1 has been taken as reference. The PV power generation has been estimated using incident angle and weather conditions. The data estimated with despatcher module has been compared by real data generated by an existing solar PV plant.

3.2.2.1. Solar panels irradiation components

The Figure 3.4 shows the total sun radiation received by the solar panel on earth surface consists of direct, diffuse and reflected beam radiations. These solar beam components are essential for the design using mathematical modeling of PV module [57]. The predicted solar power and real PV panel power has been compared within despatcher module.

It has been reported that panel predicts and estimate the power maximization when the angle between solar rays and panel is 90° . The output maximization has been reported using single-axis as well as double axis tracking systems.

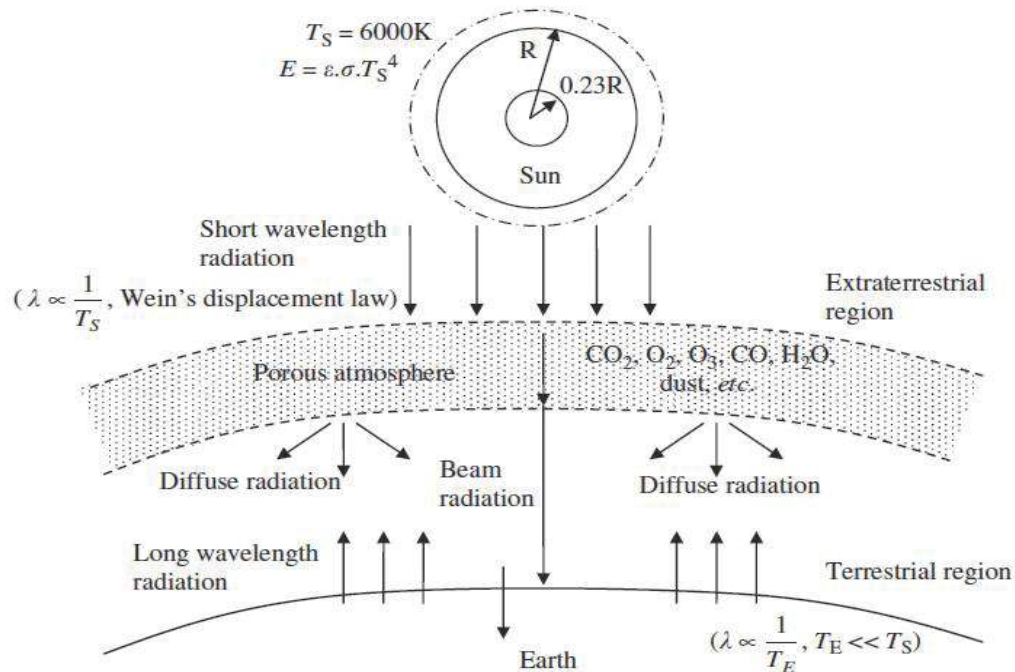


Figure. 3.3. Sun position and the Solar Radiation components [58]

The most common approach to optimize the solar power is to install the panel tilted with south direction, and during various experiment it has found that the power is optimized with 71% with dual axis tracker system, where, the 29% loss in the power is easily offset by tighter installing panels so that fixed installation of solar panels is the most appropriate [57]. When the solar panel is fixed, angle of incidence is not optimal and changes over time. This results in a change of the total irradiation components and the total power generated by the solar panel. To estimate the solar plant electricity generation we must compute components of sun irradiation. All this radiation values can be computed based

on direct beam radiation, solar altitude angle, sky diffuse factor, incident angle, tilt angle and reflection coefficient of surrounding surface.

Computation of elements of sun radiation has been estimated based on direct beam radiation, solar altitude angle, sky diffuse factor, incident angle, tilt angle and reflection coefficient of the surrounding surface. Angles of installation, sun position, air and surrounding characteristics are constants and can be defined for target position and has been derived from Table 3.1 Angles of installation, sun position, air and surrounding characteristics are constants and can be defined for target position, but direct beam insolation varies during year and special model for its computation has been used and values of radiation components was computed for the direct beam insolation propagation exist model developed in USA by American Society of Heating, Refrigerating and Air Conditioning Engineers (ASHRAE model) and MEINEL model, are referred.

Table 3.1. Solar Insolation Components calculation [58]

Type of radiation	Governing equation	Remarks
Beam Radiation on the horizontal surface I_{BH}	$I_{BH}=I_B \sin\beta$	β is the sun altitude angle
Diffuse insolation on the horizontal surface I_{DH}	$I_{DH}=C.I_B$	C is the sky diffuse factor
Total horizontal insolation I_H ,	$I_H=I_{BH}+I_{DH}$	
Beam insolation on the collector I_{BC}	$I_{BC}=I_B \sin\zeta$	ζ is the incident angle.
Diffuse insolation on the collector	$I_{DC} = I_{DH} \left(\frac{1 + \cos\Sigma}{2} \right)$	Σ is the tilt angle
Reflected insolation on the collector	$I_{RC} = \rho.I_H \left(\frac{1 - \cos\Sigma}{2} \right)$	ρ is the reflection coefficient of the surrounding

The American Society of Heating, Refrigerating and Air Conditioning Engineers (ASHRAE) model and MEINEL model has been used for the comparison of beam components. The value of solar insolation components has been computed as per equations stated in Table 3.1 and Table 3.2.

Table 3.2. Comparison between established ASHRAE and MEINEL models[58]

ASHRAE Model	MEINEL Model
Direct beam radiation equation $I_B = Ae^{-k.mr}$	Direct beam radiation equation $I_B = 1353 * 0.7^{AM^{0.678}}$
Where A is the apparent extraterrestrial flux and $A = 1160 + 75 \sin \left[\frac{360}{365} (n - 275) \right]$	AM is the air mass and 0.678 the empirical constant computed for USA conditions and for any geographical locations.
k=optical depth, $k = 0.174 + 0.035 \sin \left[\frac{360}{365} (n - 100) \right]$	where the value of 1353 W/m ² is the solar constant
'mr' is the air mass ratio, and 'n' the year day number,	0.7 the share of solar irradiation that reaches earth surface.

3.2.2.2. Sun Position Angles Estimation

The maximum power output has been based on sun position, defined in the horizontal coordinate system as sun height (altitude) and sun azimuth angles as shown in Figure 3.4. The astronomy based simple and accurate Earth movement model has been referred for the sun coordinates [59].

The sun position computation has been written using MATLAB language function. To calculate sun coordinates at any time for any day, a reference date is defined as 1st January 2000 and any day number can be calculated from calendar formula [59] as given in Equation 3.1.

$$d = 367 * Y - \frac{7 \left(Y + \left(\frac{M + 9}{12} \right) \right)}{4} + \frac{275 * M}{9} + D - 730530 \quad (3.1)$$

Where 'd' is the day number (integer) from 1st January 2000, 'Y', 'M', and 'D' denotes the year, month, and the day of the observation respectively. Using any day number various sun orbit parameters have been computed and the rectangular coordinates of sun in the plain ecliptic have been located.

The azimuth and altitude solar angles has been computed using the Table 3.3 in the terms of specific date, month, year, hour, minute, second, latitude, longitude and time difference from Greenwich meridian.

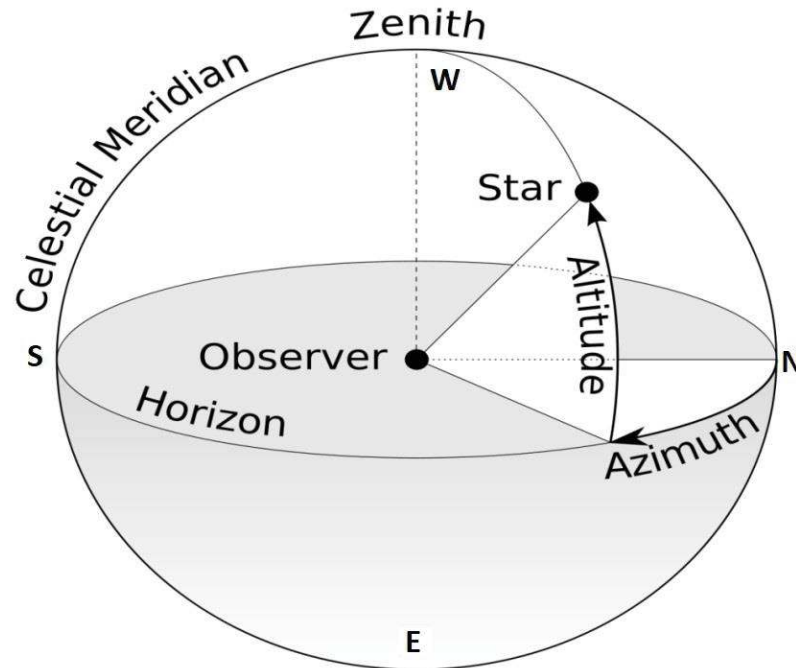


Figure. 3.4. Horizontal coordinate system [60]

This paragraph has attempted to bring more clarity on the tables containing equations. The day number is an integer value. Using day number we can compute sun orbit parameters for this date, main parameters of the orbit are longitude of perihelion, eccentricity and mean anomaly, which gives input to the calculations for Sun's mean longitude. Next, we could compute an auxiliary angle, eccentric anomaly, using standard reference given. Further rectangular coordinates of sun were calculated in the plain of ecliptic, the X axis points towards the perihelion. Next step is calculation of side real time, side time is a local time which is computed. To compute the altitude and azimuth we also need to know the hour angle. The hour angle is zero when the celestial body is in the meridian i.e. in the south – this is the moment when the celestial body is at its highest above the horizon.

Finally, we compute azimuth and altitude. This method of solar angles computation let us compute the sun height and azimuth of the sun for a date, month, year, hour, minute, altitude and latitude, and the time difference from meridian. Thus for any point on the Earth's surface at any given time, we can determine the coordinates of the sun angles.

The usage of equations in Table 3.3 has been used in MATLAB codes.

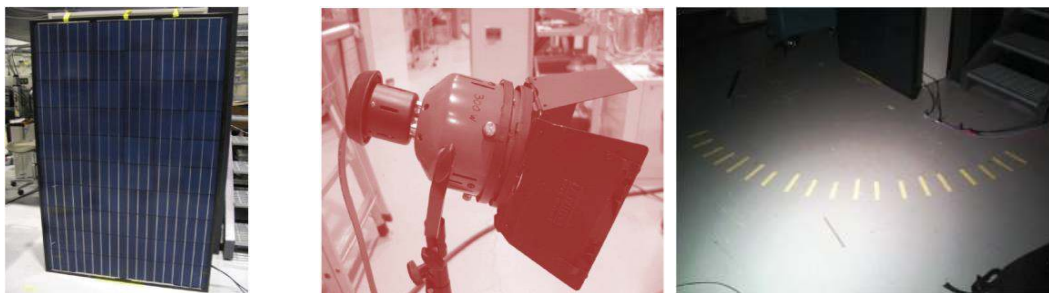
Table 3.3. Time / Date Dependence of Sun Orbit Parameters [59]

Parameter	Equation
Longitude of perihelion 'w'	$w = 282.9404 + 4.70935 * 10^{-5} d$
Eccentricity 'e'	$e = 0.016709 + 4.70935 * 10^{-5} d$
Mean anomaly 'm'	$m = 356.0470 + 0.9856002585 d$
Obliquity of the ecliptic 'oblecl'	$oblecl = 23.4393 - 3.563 * 10^{-7} d$
Sun's mean longitude 'L'	$L = w + m$
Auxiliary angle and Eccentric anomaly 'EA'	$EA = m + \left(\frac{180}{\pi}\right) e \sin m (e \cos m)$

3.2.3. Experimental analysis for Height and Azimuth angles

An experimental analysis has been carried out at location 1 for the power estimation based on sun movement. A standard 230 W solar panel has been insulated using 300 W halogen lamp. 5° step azimuth angles data had been collected for 90°, 95°, 100°, 105°, 110°, 115°, 120°, 125° and 130° sun height angles as presented in Figure 3.5. (a), (b) and (c). To find out dependencies of solar panels on sun position and weather conditions tests were conducted with real solar panels at location1 both in the laboratory and in real conditions. In laboratory incident angle were specified manually, but for real test defined the dependency of sun position angles on date and time. So for measured data analysis block of estimation of sun position in the defined date and time have designed.

Solar panel voltages were measured by a data acquisition system, where the voltmeter is connected directly to panel without load [61]. The experiment the solar panel voltage measurements was done every 5° change starting from 90° height angles, and measured values of azimuth angles from 0° to 90°.



(a) Solar Panel-230W (b) Lamp of 300W (c) Lamp positions to panel

Figure. 3.5. Experimental setup for estimation of sun angles at location 1

Solar panel voltage at different azimuth angles for 90° sun height has been presented in Figure 3.6 and it could see that the solar panel voltage reaches its maximum at 90° azimuth angle and decreases with azimuth tends to 0°. At 0° azimuth angle, the solar panel voltage is not '0' V, because of influence of the diffused and reflected irradiation components. It is also reported that generated power of the solar panel is proportional to square of voltage and dependency of the photovoltaic panel power on the azimuth angle [57].

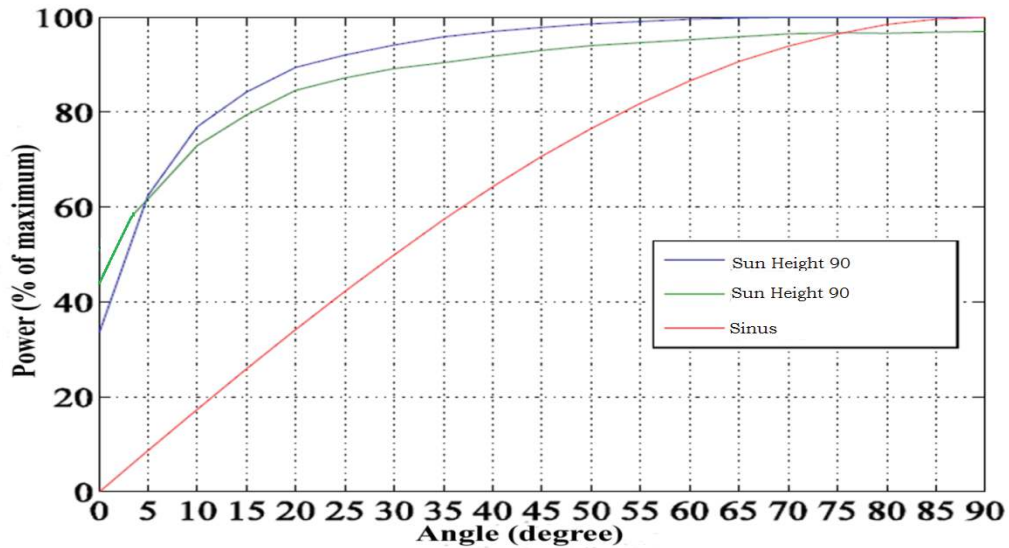


Figure. 3.6. Dependency of the PV panel power on the azimuth angle

The real data has been collected from the existing 1200W PV system fixed with inclination of 18.4 degrees and azimuth angle of 78 degrees. Accordingly, the sun azimuth and height angles have been estimated. This real solar generated power at location 1 on the 19th June 2017 is shown in Figure 3.7.

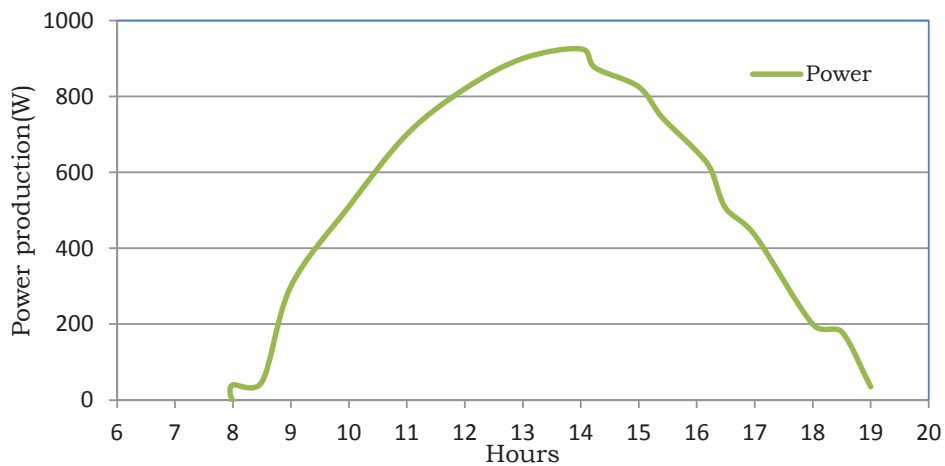


Figure. 3.7. PV power generation for the 19th June 2017

3.2.4. Influence of Sun Angles for Solar system output

As the panel output varies with sun position angles, sun altitude and it reaches to a maximum value at 90° azimuth angle. During the day time, both sun angles changes instantly, but generation does not depend only on the sun height angle or azimuth angle, but also on the angle between the solar beam and solar panel surface [62].

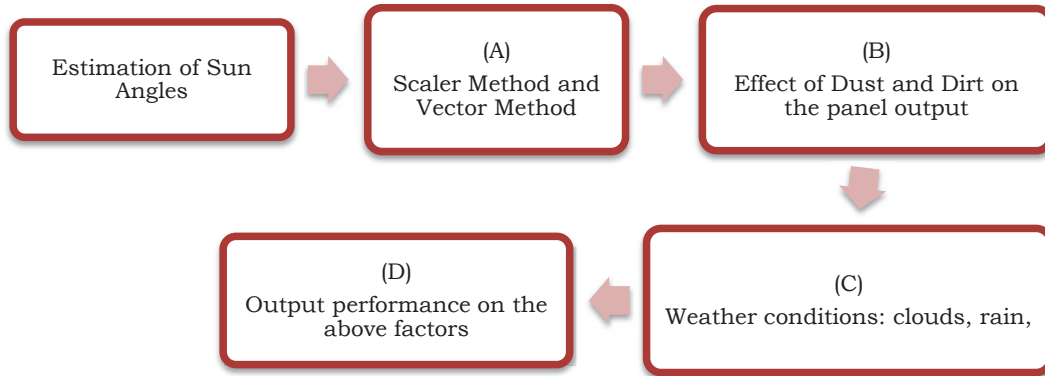


Figure. 3.8. Flowchart for the performance output of Solar Panel

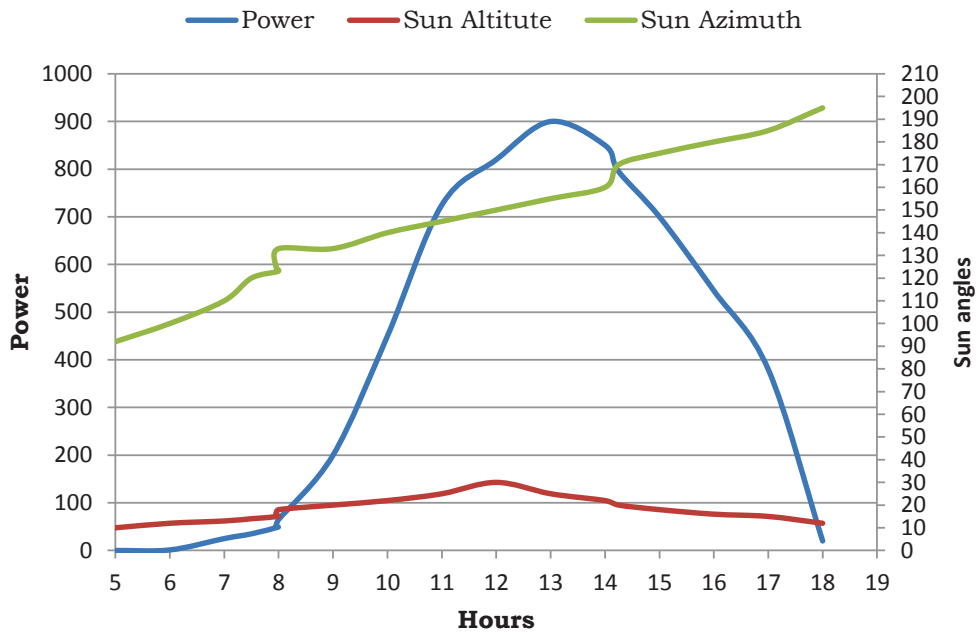


Figure. 3.9. Sun position angles and PV power generation

The PV panel performance for various parameters has been estimated using MATLAB model following the progress flowchart in Figure 3.8. The MATLAB code for various sun angles, solar power estimation and generation has been

simulated and results are shown in Figure 3.9 and Figure 3.10 respectively. The logic, equations and cases has been used in MATLAB codes.

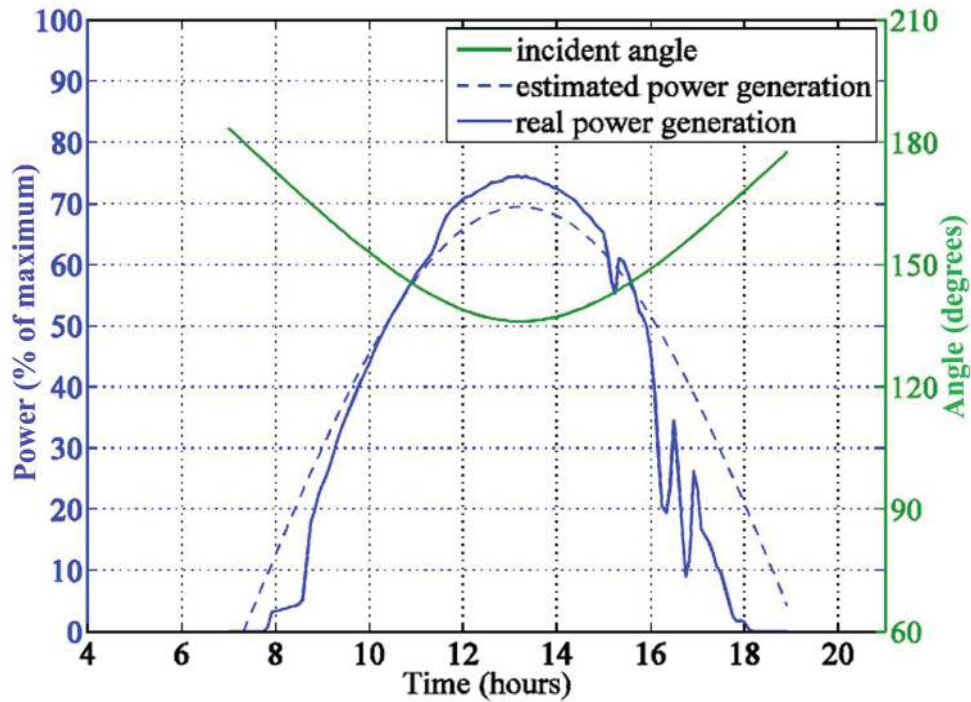


Figure. 3.10. Comparison between real and estimated generation

3.2.5. Effect of Dust, Clouds and Rain on the panel output

Other factors by which the solar power output gets affected are effect of dust or dirt, deviation due to weather conditions (cloud and rain). The designed dispatcher would predict and estimate the panel output in real conditions, with major data factors of dust, clouds and rain dirt. It has been reported that the losses on the account of dust reaches more than 25% of irradiation power for low sun angles and 5% at maximum panel-sunbeam angles. In present work, power losses by clouds and rain have been considered using '*feedback coefficient*' which is actually ratio of the measured power value and estimated the same time instance [63]. To control the deviation of the estimated value this coefficient has been checked and corrected every one hour. In literature, the diffused irradiation on the collector is estimated and it depends on the beam irradiation, sky diffuse factor and cosine of tilt angle as mentioned in Equation 3.2

$$I_{DC} = 0.25 * (0.9 * \frac{CC}{100} * I_B * \sin \beta) \quad (3.2)$$

where CC is the total cloud coverage in percent.

The Figure 3.11 shows the primary simulation results under such conditions.

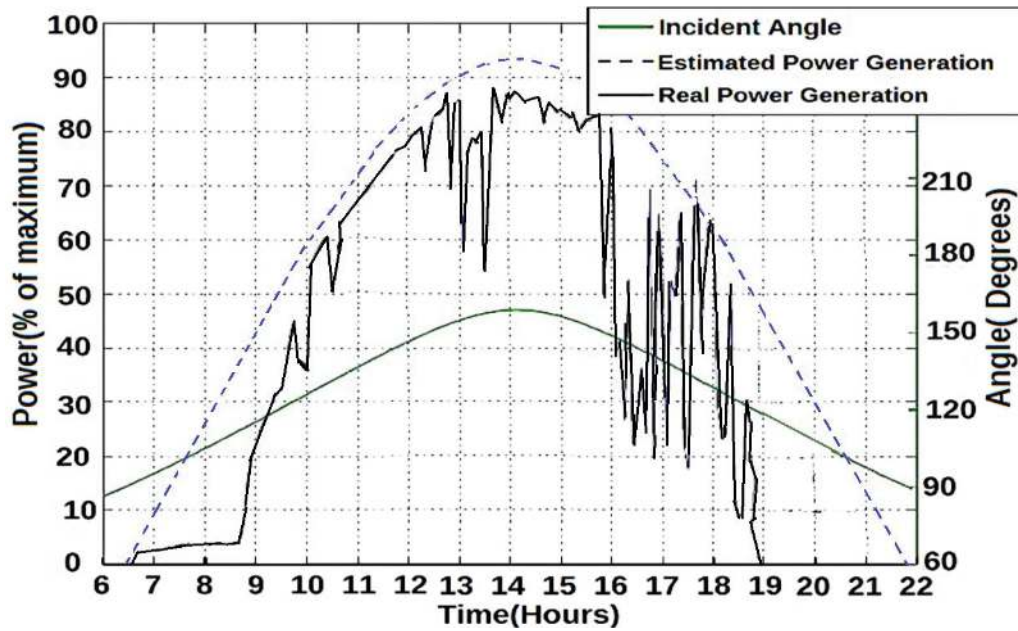


Figure. 3.11. Measured and estimated data in percent of P_{MAX}

Power generation depends on cloud density and mean coverage of sky by clouds. Modern weather prediction systems using national metrological website has been used to deliver high precise forecast of cloudiness and the amount of precipitations for every hour.

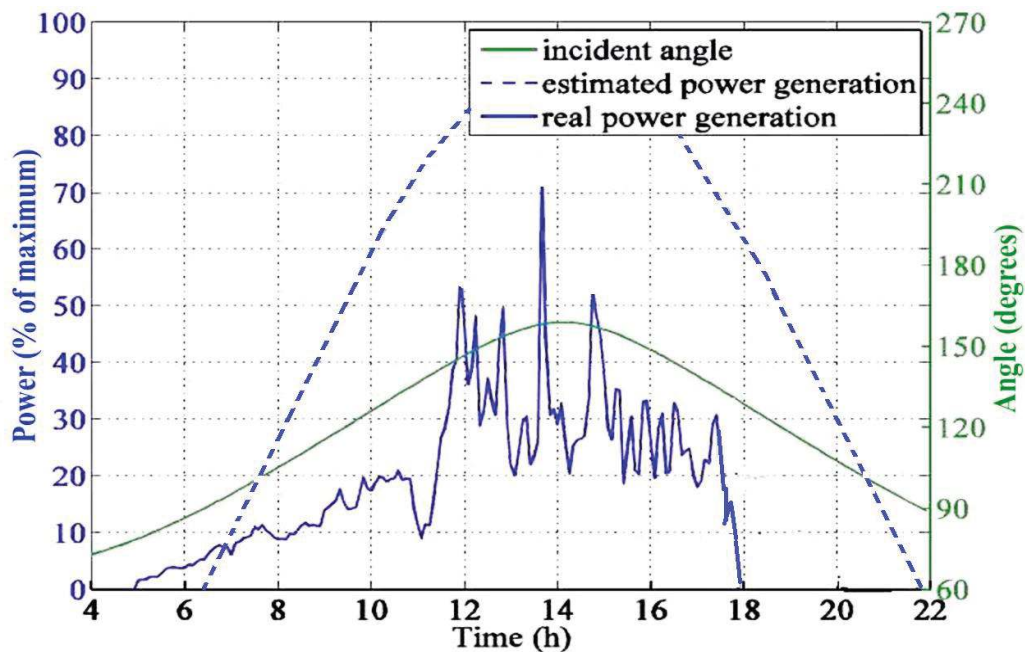


Figure. 3.12. Effect of clouds/sunset on measured and estimated values

The method of solar angles computation a generic and standard formulae has been derived and MATLAB code is generated to compute the sun height and azimuth of the sun for a date, month, year, hour, minute, altitude and latitude, and the time difference from meridian. Thus, for any point on the Earth's surface at any given time, we can determine the coordinates of the sun. The study was conducted at a real oil and gas site located at north east of India and one mid-summer day it was noticed that sun rises at 0400 am, accordingly author thought to extend the estimation as general cases assuming if days are longer and even after the diffused radiations also contributes the solar power production.

The simulation Figure 3.11 shows the fluctuating power drop from 1600 and 1800 hours mainly due to clouds and rains. This means that the water, that covers panel surface after the rain, plays the great role in power losses and rain influence on the diffused and direct irradiation separately. The results have been shown in the Figure 3.12. During rain, water diffuses and absorbs light in the air and covers the solar panel surface and finally the output drops drastically. This water coverage also affects the solar diffusion and it is also seen that heavy rain affects the generation up to 90% of the capacity.

The model has been tested for real situations based on effects of cloud and rain. The results in Figure 3.11 and Figure 3.12 could also be extended to any position of solar panel based on its latitude and longitude, as the very early rise of sun at location 1 was studied. The accurate solutions and graphs has been discussed in the results in Chapter 5.

3.2.6. Module realization description

To realize the estimation of PV power generation, MATLAB functions have been written for each element of SIMULINK model and shown in Appendix A. The MATLAB code and their relevance has been summarized in the Table 3.4

Table 3.4. Module MATLAB Code realization

Matlab Code	Concept and Relevance
Sun_Angle	Calculates the sun altitude and azimuth angles.
Vec_Angle	For better accuracy 'Vector method' for sun angles calculates the angles between vector pairs. It calculates the angle between each pair of vectors from different matrices.

Day_Irradiation	Calculates maximum diffuse, direct irradiation components every minute for sun altitude and azimuth angles
Power	Estimates the PV power generation with dynamic weather forecast as a function of the maximum power, maximum possible diffuse and direct irradiation components

3.2.7. Power Consumption Propagation

The objective of the dispatcher is to minimize grid power usage and decrease total energy consumption cost. However in some situations, because of unused solar panel power, some part of energy consumption will not be controlled by system. It means that to estimate unused solar panels energy one need to propagate future uncontrolled power consumption. In this section a comparison of existing methods of power consumption propagation [64] has been summarized in Table 3.5 and chosen the method, which fits the conditions.

Table 3.5. Comparison of Power Consumption Propagation methods

Method	Relevance
Conventional : Linear Model Prognosis of electricity consumption	
<ul style="list-style-type: none"> ❖ Earliest developed methods[65]. ❖ Regression based analysis, where load is modeled as function of previous values. ❖ Autoregressive, dynamic linear or nonlinear, load as a function of several external factors including weather[66] 	<ul style="list-style-type: none"> ❖ Widely used as linear regression models, despite of various alternatives. ❖ The nonlinear function series model on the load, work on exogenous variables.
Intelligent : Artificial Neural Networks(ANN) & Fuzzy[67]	
<ul style="list-style-type: none"> ❖ Theory of artificial intelligence (AI), ANN, Fuzzy Logic(FL), Genetic Algorithm (GA) ❖ Multilayer ANN networks in the offline back propagation mode. ❖ Network with variable number of neurons in the hidden layer [68] ❖ FL allows the propagation which is not possible for the prediction in ANN. ❖ Forecast the electrical load every hour 	<ul style="list-style-type: none"> ❖ Ability load forecasting and diagnose neural networks for complex sequence ❖ Fuzzy logic is difficult and best reflects all the processes influencing the fluctuations of consumption. ❖ Fuzzy predictive model estimation with result

and compares continuously	accuracy of about 5%.
Hybrid: Two or more different models to improve the forecasting, and to automate the procedure of constructing the forecast (ANN + FL) or (ANN+ GA)	
<ul style="list-style-type: none"> ❖ Predict the load on the day or week ahead with a FL weather conditions opting many layers of ANN model. ❖ Neuro-systems which combine with the advantages of ANN and FL, and are able to automatically generate a fuzzy system from the neural network [69]. ❖ The genetic algorithms (GA) optimizes the developed prediction and describe the evolutionary approach to learn and adjustment of artificial neural networks. 	<ul style="list-style-type: none"> ❖ Accuracy ranges from 3-7%, the accuracy of neuro predictor is within 2–3%. ❖ Weather sensitive elements. ❖ GA method is used of previously proposed state estimation of power systems and telemetry verification. Further GA is used in the optimization of energy systems by the active power.

The Table 3.5 briefed the propagation methods for the power consumption however, majority of these methods are complicated and their algorithms demands lot of time. Since present work has been oriented on a small (6MW) power plant, with quite low power requirement, such complicated methods and algorithms are not suitable considering their cost effectiveness and efficiency.

The simplest Linear **Moving Average (MA) model** has been chosen to estimate the uncontrolled consumption[70]. The future power consumption for day cycle for every week day equals to the mean power consumption cycle. The power measurement cycle must be high enough to detect the power consumption of devices with small working time, for example air compressors, but not too high to bound amount of saved data.

To estimate the mean uncontrolled consumption one need subtract controlled by system power consumption data from the total consumption data. Resulting uncontrolled consumption data need to be send to the consumption prediction module where will be computed the mean consumption for week day.

3.2.8. Despatcher Module Design

This section gives a brief idea on the working methodology of the despatcher module, its main data structures and implemented routine module. The detailed control system test results have been presented in the Chapter 5. Since this

chapter was a brief introduction on three multidisciplinary areas, a brief has been given.

The data calculated in the solar power propagation and uncontrolled consumption propagation blocks must be collected by a despatcher block as shown in Figure 3.2, which operates as the main function of the control system (control of energy consuming devices). This data has been used for the estimation of the amount of free solar energy for the decisions of despatcher. This data enables the estimation of potential work times of the devices, analysis of these times and choice of the most convenient for the chosen criterion. The amount of free solar energy can be computed as a difference between the estimated solar power generation and uncontrolled prognosis.

The preciseness of free solar energy helps despatcher for best decisions. The uncontrolled consumption propagation block realized in the system is very easy and does not depend on the external conditions, and so prognosis do not changes with time.

The external factors dependency of the solar power prognosis provokes need to refresh and improvement of the propagation result. The main factors for the deviation are the weather forecast dependency. The weather forecast can change during the day long, and the estimated solar panel power must change too. Solar power propagation block has been called every hour not only ones in the beginning of the day, but repeatedly during the day. This time period must be decreased to guarantee usage the most actual weather information.

Devices divided into two groups have categorised with different control parameters. For 1st group devices control parameters are maximum and minimum values of measured value. For the 2nd group devices the control parameters are work cycle of the device and owner specified desired due time of the work execution. Devices from both the groups have a common parameter which is power consumption in Watts. This value estimates the influence of the device on the amount of free solar panel energy. For the devices, which power consumption changes with time (mostly second group devices) the greatest value must be indicated to analyse the worst case. The device, their time cycle and their effect on output has been discussed and shown in the chapter 5.

3.3 Substitution of NG with CSP for Crude Oil Heating Applications

In the last chapter, the concept of CSP has been proposed for industrial applications and supports for the energy security. This work has been focused on specific oil heating applications and emerged that CSP technology has large potential to mitigate the emissions and maintain energy security.

3.3.1. Research Concept and Platform

The typical schematic of any oil and gas installation termed as Group Gathering System (GGS) has been demonstrated in Figure 3.13. It has been shown that crude oil (also termed as Emulsion²) passes through a chain of processes and also ‘Heater Treater’. In this heating chamber, fire tubes are extended and which are submerged in emulsion oil. The heating decreases the viscosity of containing oil and water, which further reduces the resistance of movement. In continuation, the surface tension between droplets reduces and formation of bigger droplets created. The heater treater system has been widely used for pre-heating of the emulsion and crude separation of oil and water. The temperature required for breaking the emulsion is around 80-85°C [71]. A mix of dispersion of any immiscible liquid into another with chemical use reduces the interfacial tension between the two liquids to achieve stability.

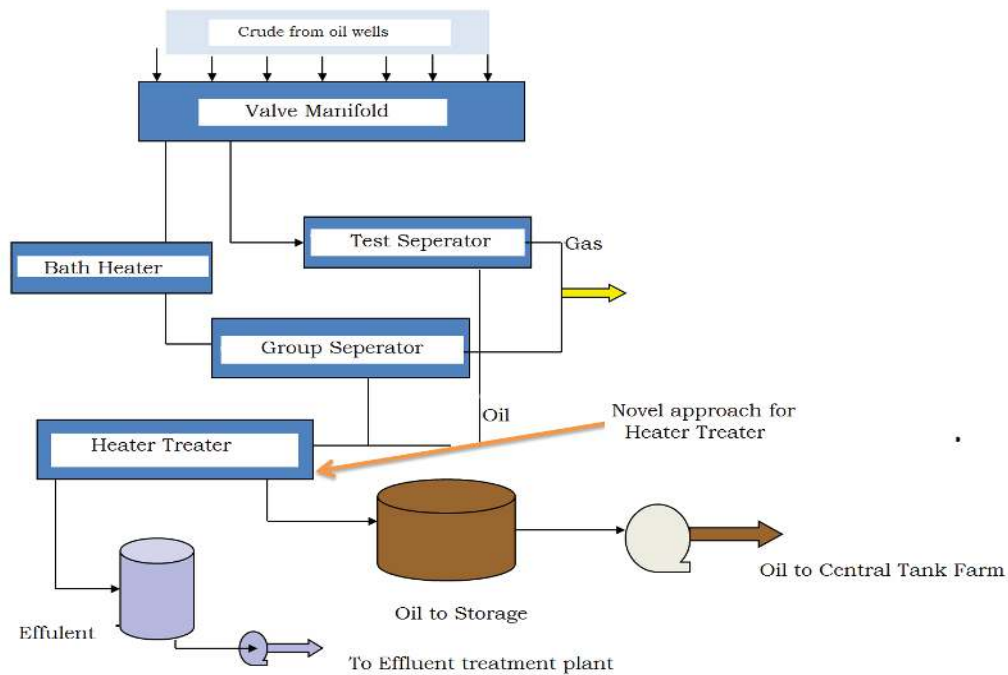


Figure. 3.13. Typical Gas Gathering System layout in oil sector [72]

² Emulsion contains Crude oil and Water in 1: 6 ratio approximately

Degassing chamber a part of horizontal heater treater system through emulsion flows and allows gas to pass away and leaves the heated emulsion next into an electrical chamber as shown in Figure 3.14. In electrical chamber the gas being lesser denser has been evacuated from top. Similarly, in electrical chamber, a water level is continuously maintained for oil washing and free water droplets are eliminated before fluid proceeds towards electric chamber. This process is called as Electrostatic Coalescence. Several small water droplets would be dispersed in the crude emulsion and would be coalesced by a high-voltage (11.1kV) electrical field. When this nonconductive crude oil is subject to electrostatic field, dispersion takes place between water droplets.

Parabolic dishes (or Sterling engines) system uses the aligned parabolic mirrors to align solar insolation onto a receiver, which is oriented at the focal point of the dish. The working fluid in the receiver heats up to very high temperatures of range 500-750°C [73]. This high temperature fluid is further utilized to generate electricity in a micro Sterling Engine, or Brayton cycle engine. The detailed crude heating process and research methodology has been elaborated at Section 4.2.1.

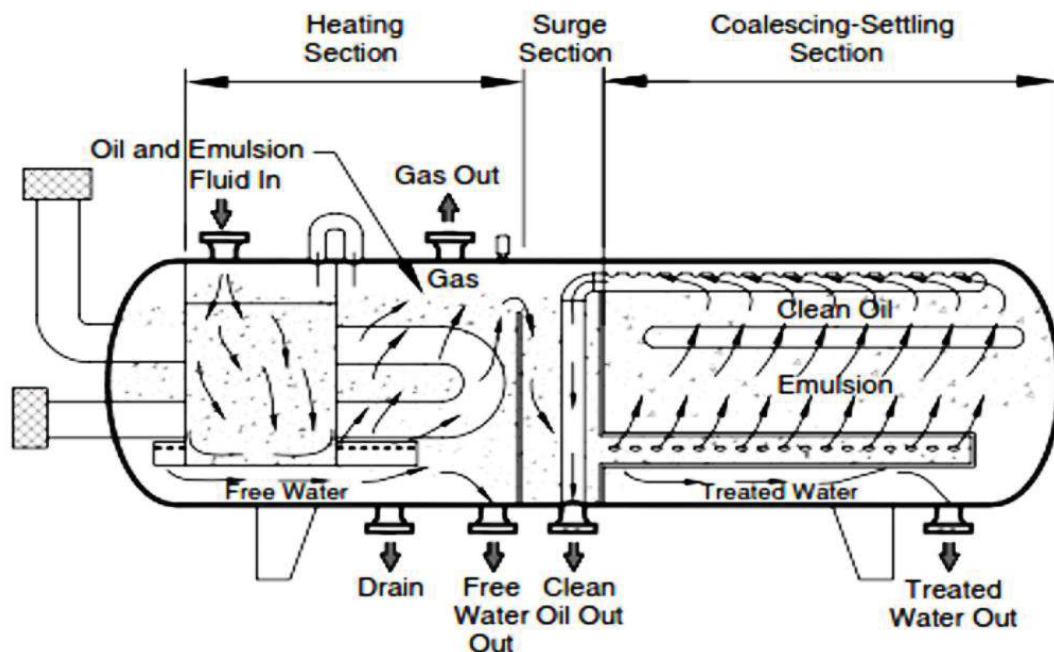


Figure. 3.14. Cross section of Horizontal Heater Treater [74]

It has been reported that among all Solar thermal technologies, dish based CSP systems are the most efficient and 25% more effective with an additional advantage of least water consumption [75].

Various other major parameters which have been considered in the design are concentration ratio for dish, optical efficiency of collectors, wind speed, heat loss and transfer coefficient, air / dish skin temperature, thermal efficiency, temperature and flow rate of oil and thermal heat.

The estimation and computations for the conceptualized prototype model utilizing the proposed solar collector has been discussed and results are drawn. The detailed calculation has been made using Appendix C. The prototype CSP dish has been developed, tested and demonstrated. The performance of solar concentrator has been found dependent upon solar radiation insolation, site condition, sunshine hours and other parameters. The detailed discussions and results have been shown in Chapter 5. In this work, a prototype has been modeled as a hybrid solution with existing natural gas fired crude oil heating facility for better reliability of continued oil processing. The technical specification of the prototype model has been chosen with the reference industrial data of a location 2 as summarized in the Table 3.6.

Table 3.6. Design parameters of prototype system [76]

Average Performance of 8 M² for Parabolic Solar Concentrator(PSC)			
Specifications (Units)	1 PSC	4 PSC	10 PSC
Aperture Area (M ²)	8	32	80
Heat Delivery Rate/day (KW)	30	90	225
Daily Energy Produced (kcal *1000)	21	89	234
Annual Sunshine (8 hrs / day)	2400	2400	2400
Annual Fuel Savings (oil, kerosene, diesel) (kg)	653	2234	5645
Steam Generation Kg/day	30	112	350
Unshaded Space M ² requirement	20	80	220
Aperture Area M ²	8	32	80
Heat Delivery Rate/day KW	24	80	225

3.4 Bio-fixation of CO₂ with microalgae in Oil Sector in India

Other Renewable Energy source Microalgae have been reported as emerging 'Biomass' to mitigate and 'Capture the emitted Carbon', which is an important aspect of Figure 1.2. This carbon mitigation theme has been rechristened as 'Bio-fixation of Greenhouse Gases (GHG)-CO₂ with microalgae'.

During last decade with research advancements, the Microalgae have been recognized as an important and potential biomass resource for the generation of renewable energy based electricity [77]. The selection of microalgae for carbon capture are based on three major aspects viz, ability to sequester carbon (in presence of sun light) emissions, potential to produce the *lipids*³ in form of hydrocarbons and multipurpose usage of algal biomass in across the industries. Algae have been reported to have major characteristics of high biomass yields per unit of solar light and surface area. Also, the cultivation of biomass doesn't need agricultural lands as well as fresh water, and this makes micro-algae the best possible renewable resource for electricity generation.

Carbon emission containing CO₂ from Industrial sources and other sources are targeted for the *sequestration*⁴ by utilizing the algal biomass [77]. This mitigation solution has been linked to build a practical industrial application at location 3. The effective cultivation of algal biomass varies with physical, biological and environmental parameters. The inherent character of selected species and geometry of production system do support the photosynthesis activity and production of biomass.

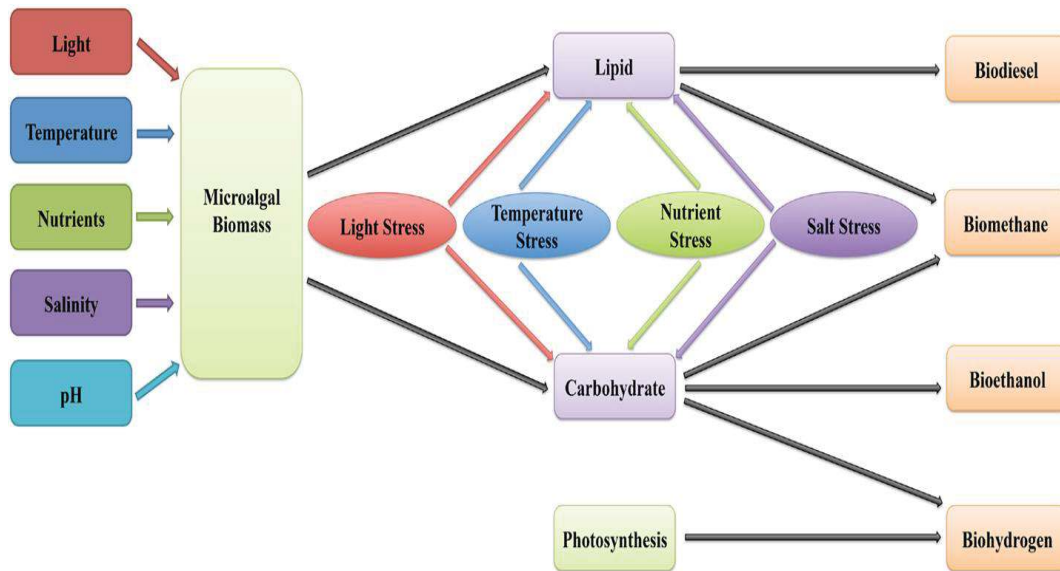


Figure. 3.15. Microalgae based co-products supply chain [78]

Incident solar light, temperature, nutrients, salinity and pH of waste water plays important role in the biomass cultivation. Figure 3.15 depicts the

³ Lipids: Liquid organic compounds that are fatty acids or derivatives, insoluble in water

⁴ Sequestration: Capturing of Carbon from environment

integrated platform the value-added products. One of advantage of direct conversion of raw algae is to carry out the anaerobic-digestion⁵ in producing CH₄ and recycling of various nutrients like sodium, potassium etc.

The industrial vent gas at location 3, containing CO₂ is targeted for biological sequestration and conversion combination of algal biomass and anaerobic digestion for biogas generation. The vent gas analysis and pilot study were carried out for the period of six months and finally suggested that the 33% initial CO₂ concentration vent gas has been reduced to an average of 15% CO₂. The entire 33% CO₂ present in vent gas can be sequestered in liquid by employing pressurized water scrubbing system and the carbonated liquid can be transported to algal ponds / photo- bioreactors set up [79].

The biogas produced has been utilized for combustion purpose and substitute the NG being used for the crude oil heating at location 2. The present crude oil heating arrangement needs some electrical power requirements and to continue with the carbon sequestration, artificial lighting equipment have been utilized for longer period of day and night time. In respect to Carbon dioxide sequestration studies and their results, it has been found that Photosynthetic algae require carbon dioxide for its growth and they also can utilize carbon dioxide in the form of soluble carbonates.

It has been reported that Biogas or Biomethane production with the combination of carbon capture with storage consists of high potential to remove a considerable amount of GHG emissions from the atmosphere. It has been also estimated that the annual GHG saving could be approximately 8 Gt by the year 2050, if natural gas based system would be replaced or hybridized with biogas production. It has been evaluated that the technical potential of algal biomass are limited with respect to the availability and selection of sustainable species and yield biomass [80].

The economic feasibility of algal biogas strongly depends upon the CO₂ price and NG price and it has been reported that the economic potential of biogas is much lower than the technical potential in several industrial scenarios. The combination of technical and economic feasibility makes this option favorable for oil and gas industries wherever the natural gas pricing are lower and existing industrial infrastructure are available.

⁵ anaerobic-digestion: In the absence of Oxygen

3.5 Conclusions

In this chapter the dependence of sun angles and dynamic weather condition on Solar PV power generation is evaluated and suggested the concept of despatcher. Further, models of CSP based ‘Crude Oil heating’ unique hybrid solution and ‘microalgae’ based carbon capture is modeled. A prototype of CSP based hybrid system has been created and analyzed comprehensively with techno-commercial aspects.

Within this scope, two hybrid solutions has been proposed for crude oil heating as (1) CSP technology and Natural Gas system and (2) PV, CSP and Algal biomass hybrid system. In the next chapter the research methodologies of two hybrid solutions have been elaborated.